# Computer simulation of the translocation of nanoparticles with different shapes across a lipid bilayer

Kai Yang<sup>1</sup> and Yu-Qiang Ma<sup>1,2</sup>\*

Understanding how nanoparticles with different shapes interact with cell membranes is important in drug and gene delivery1-4, but this interaction remains poorly studied3. Using computer simulations, we investigate the physical translocation processes of nanoparticles with different shapes (for example, spheres, ellipsoids, rods, discs and pushpin-like particles) and volumes across a lipid bilayer. We find that the shape anisotropy and initial orientation of the particle are crucial to the nature of the interaction between the particle and lipid bilayer. The penetrating capability of a nanoparticle across a lipid bilayer is determined by the contact area between the particle and lipid bilayer, and the local curvature of the particle at the contact point. Particle volume affects translocation indirectly, and particle rotation can complicate the penetration process. Our results provide a practical guide to geometry considerations when designing nanoscale cargo carriers.

Nanoparticles are promising imaging materials and can deliver drugs, proteins and other molecules into cells<sup>1–5</sup>. However, there have also been reports of toxicity<sup>6,7</sup>. Using nanoparticles in biomedical applications involves the cellular uptake of particles. Indeed, understanding the physical penetration of particles could have huge implications in biomedical applications<sup>8–15</sup>, providing insight into the nature of endocytosis and nanoparticle–cell interactions<sup>16–19</sup>. Unfortunately, the two main translocation pathways (active and passive physical penetration) remain poorly understood. Little is known about the influence of nanoparticle geometry on the translocation process, although it has been shown to be important in various biological processes<sup>3,5,20–23</sup>. Anisotropically shaped nanoparticles can now be created<sup>24</sup>, so designing nanoparticle carriers with optimal shape and volume is becoming increasingly important.

We have simulated the interaction between nanoparticles having different geometries and a lipid bilayer using dissipative particle dynamics (DPD; see Methods and refs 25–28). DPD is one of the most common coarse-grained methods for studying biomembrane systems. It can reproduce accurate dynamic behaviour of the lipid bilayer, and can be used to explore interactions between the membrane and proteins (or particles). By varying the shape of nanoparticles having the same volume, or by varying the volume of particles with the same shape, we show that nanoparticles with different shapes penetrate the lipid bilayer differently (Supplementary Fig. S1).

To clarify the shape-dependent effect, we first chose ellipsoidal particles with three axes ( $L_{\rm a}$ ,  $L_{\rm b}$  and  $L_{\rm c}$ ; Fig. 1a). In the experiments, penetration of the nanoparticles across the bilayer was always aided by an external force 10,14,15,17,18. A driving force was therefore applied to the particle centre of mass to realize its penetration, and the minimum required driving force (Fig. 1b) was measured to estimate the penetrating capability of the particle: the smaller the driving

force required, the easier the penetration. From Fig. 1b, we find that the shape effect of small particles ( $V = 2.14 \text{ nm}^3$  with  $L_{\rm b} = 0.8 \text{ nm}$ ) is minor. However, with increasing particle volume ( $V = 17.15 \text{ nm}^3 \text{ with } L_b = 1.6 \text{ nm or } V = 141.48 \text{ nm}^3 \text{ with }$  $L_{\rm b} = 3.2$  nm), this effect becomes more obvious. The forces required increase with larger aspect ratio  $L_{\rm a}/L_{\rm c}$  due to the concomitant increase in the contact area between the particle and lipid bilayer. However, for  $L_a/L_c > 1$ , increasing  $L_a/L_c$  further has a reduced effect on the required force, which is seen to rise at a reduced rate (Fig. 1b). Particles with the ratio  $L_a/L_c$  and its inverse have the same shape, although different orientations, with respect to the bilayer plane. However, their translocation modes as well as the required forces differ. From Fig. 1c,d, it can be seen that the particle will rotate itself during the translocation process, particularly when  $L_a/L_c > 1$ , indicating that particle orientation is also a crucial factor. This orientation dependence has also been shown experimentally by Champion and colleagues<sup>22</sup>.

Further effects of particle orientation and rotation could be revealed by examining the translocation processes of an ellipsoidal particle with different initial orientations,  $\phi_0$  (Fig. 2a). As  $\phi_0$ varies from 0° to 90°, particle penetration becomes more difficult (Fig. 2b, green line) and time-consuming (Fig. 2c). Furthermore, we find that there are two rotation processes taking place during particle penetration (Fig. 2c; see also Supplementary Movies S1-S4). The first rotation occurs just as the particle begins to contact the bilayer due to the resistance of the bilayer. As the penetration proceeds, however, a second rotation follows. At this stage, the lipid bilayer is strongly deformed by the embedded particle. Under the influence of the interplay between the driving force and the elastic deformation of the bilayer, the long axis of the particle is compelled to be as perpendicular as possible to the bilayer plane. The occurrence and effect of the two rotations are closely related to the initial orientation of the particle (Fig. 2c). For example, when  $\phi_0 = 0^\circ$ , the first rotation dominates, although the degree of rotation is small. However, when  $\phi_0 = 90^{\circ}$ , only the second rotation occurs. For comparison, Fig. 2b also shows the corresponding translocation processes obtained while preventing particle rotation (red line see Supplementary Methods). We find that the first rotation hinders particle penetration, but the second facilitates penetration, particularly when  $\phi_0 = 0^\circ$  and  $90^\circ$ . For other anisotropic particles, similar rotation effects were found (Supplementary Fig. S2 and Table SII). Rotation is also affected by the location of the driving force acting on the particle; changing this can effectively control the rotation and penetrating capabilities of the particle (Supplementary Fig. S3).

Based on the above results, it can be concluded that the contact area between the particle and the lipid bilayer has an important influence on their interaction. Because the contact area between

<sup>1</sup>National Laboratory of Solid State Microstructures, Nanjing University, Nanjing 210093, China, <sup>2</sup>Center for Soft Condensed Matter Physics and Interdisciplinary Research, Soochow University, Suzhou 215006, China. \*e-mail: myqiang@nju.edu.cn

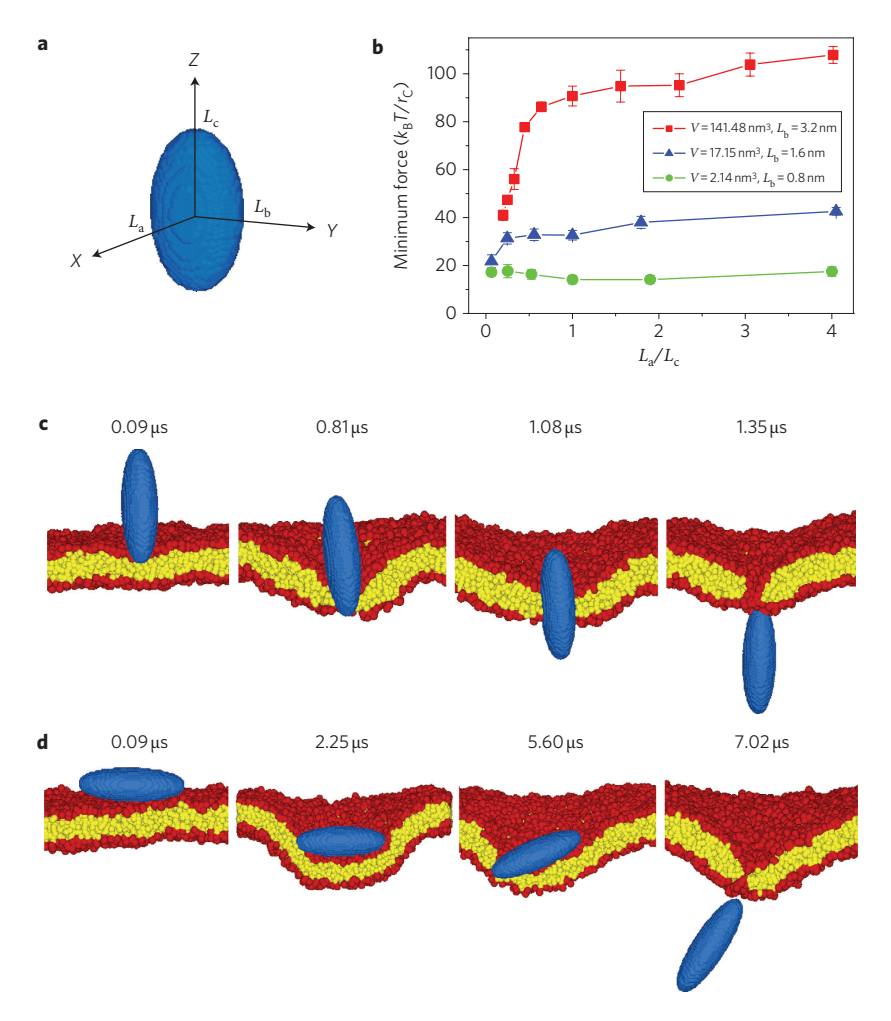


Figure 1 | Penetration of ellipsoid nanoparticles having different shapes across a lipid bilayer.  $\mathbf{a}$ , Schematic showing an ellipsoid particle, where  $L_{\rm a}$ ,  $L_{\rm b}$  and  $L_{\rm c}$  are half-lengths of three axes.  $\mathbf{b}$ , Plot of the minimum driving forces required to realize ellipsoids of different volumes through the lipid bilayer. The shape anisotropy of the particles is adjusted by varying the aspect ratio ( $L_{\rm a}/L_{\rm c}$ ) at fixed  $L_{\rm b}$  and volume.  $\mathbf{c}$ ,  $\mathbf{d}$ , Computer-simulated diagram showing the translocation of ellipsoids with vertical ( $\mathbf{c}$ ) and horizontal ( $\mathbf{d}$ ) starting orientations.  $L_{\rm a}=1.6$  nm,  $L_{\rm b}=3.2$  nm and  $L_{\rm c}=6.4$  nm,  $L_{\rm b}=3.2$  nm and  $L_{\rm c}=1.6$  nm ( $\mathbf{d}$ ). Blue, ellipsoid; red, lipid heads; yellow, lipid tails.

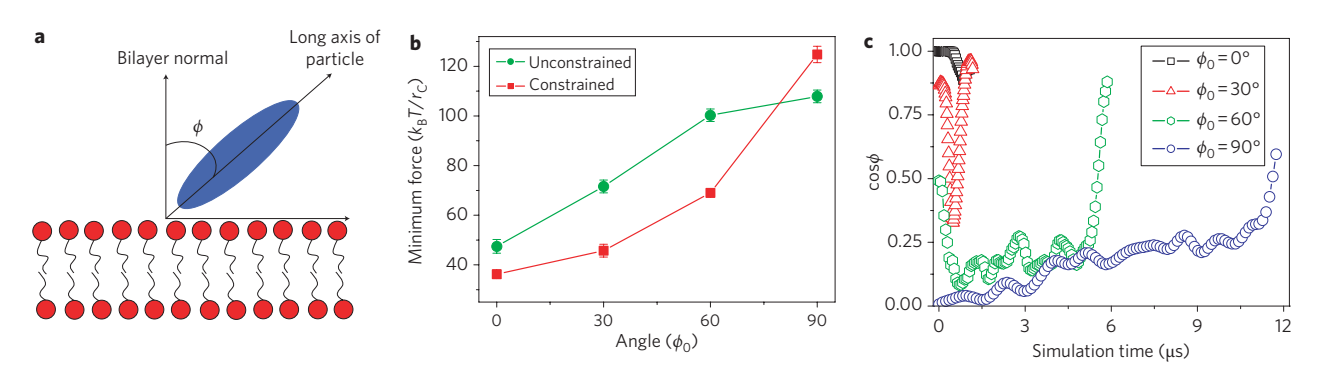
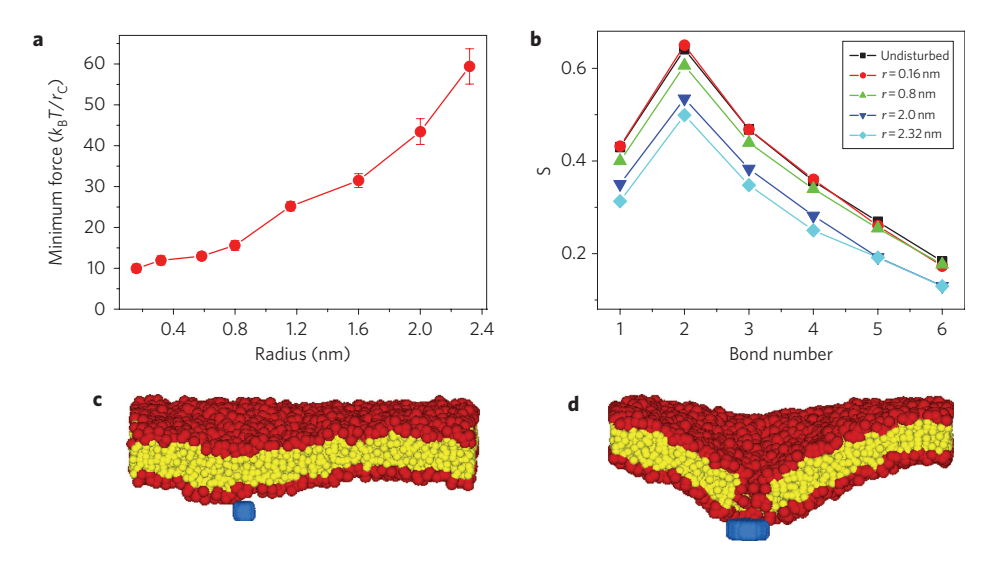


Figure 2 | Effect of initial orientation and rotation of the particle on penetration. a, Schematic showing the angle ( $\phi$ ) between the long axis of the particle and the bilayer normal. When t=0,  $\phi=\phi_0$  (blue, particle; red, lipid heads). b, Minimum driving forces required to guide the ellipsoid ( $L_{\rm a}=1.6$  nm,  $L_{\rm b}=3.2$  nm and  $L_{\rm c}=6.4$  nm) with different initial orientations of the long axis through the lipid bilayer. 'Constrained' refers to the case where the rotation of the particle is fixed, whereas 'Unconstrained' refers to the case where the particle can rotate freely during the penetration process. c, Time evolution of particle orientations during the ellipsoid penetration processes with different initial orientations,  $\phi_0$ . Each trace represents a whole penetration process of the particle.

the particle and the lipid bilayer is essentially equal to that of a disc plane when the particle is parallel to the bilayer during penetration, the effects of contact area can be examined by introducing disc-shaped particles. From Fig. 3a, it can be seen that particle

penetration becomes more difficult with increasing contact area. When the particle radius is small (for example, <0.8 nm), its influence on penetration is small (Fig. 3c). However, when the radius is large enough, a 'hydrophilic hole' is formed along the



**Figure 3** | **Effects of contact area on particle penetration. a**, Graph showing minimum driving forces required for disc-shaped particles with different radii to translocate across the lipid bilayer (disc height, h = 0.8 nm). **b**, Change in the lipid packing order, S, when discs with different radii just past across the lipid bilayer. Larger discs disrupt the order of the bilayer, causing parameter S to be smaller than the undisturbed bilayer. **c,d**, Computer-simulated snapshots of a particle (blue) just passing through the lipid bilayer for discs of radius r = 0.8 nm (**c**) and 1.6 nm (**d**).

particle translocation pathway (Fig. 3d), although it can quickly reseal. The effect of the contact area can also be revealed by the order parameter  $S = \langle (1/2)(3\cos^2\theta - 1) \rangle$ , where  $\theta$  is the angle between the neighbouring bonds in the lipid chain, and S can therefore be used to express the packing orientation of lipids in the bilayer. Figure 3b shows that when the particle just passes through the bilayer, discs with small radii have only a minor influence on the packing states of the lipids (that is, the change in S is small). However, when the disc radius is large, the lipids become clearly disordered (S becomes smaller). It is therefore possible that discs with a smaller contact area will have lower cytotoxicity because they cause less disruption to the bilayer.

Because the disruption area of most particles is not always equal to their maximum possible contact area, it is crucial to understand the influence of varying the contact area of particles on the penetration process. Here, three types of particles are taken into account (Fig. 4a). The first two types of particles were constructed by halving an ellipsoid ( $L_a = L_b = r$ ,  $L_c = h$ ), and were used to model the gradual increase and decrease of the disruption areas, respectively (with particle rotation fixed). A cylindrical particle was used for comparison. Figure 4b shows that penetration becomes more difficult when the maximum possible contact area of the particles increases (that is, increasing r at fixed h). However, the local curvature of particles at the contact point has a strong influence on particle penetration. Indeed, when the disruption area of the particles gradually decreases or remains constant during the translocation process, the change in the required force is small as particle height increases; however, when the particle disruption area gradually increases, the force will obviously decrease as particle height increases, especially for large particles. The maximum possible contact area and the local curvature of the particle are therefore both important in determining particle penetration. Note that there is a tiny glitch in the force when h is  $\sim$ 1.5 nm. This may be caused by the change in the contact between the particle and the hydrophobic part of the lipid bilayer (the thickness of the hydrophobic part is  $\sim$ 1.2–2.0 nm).

Particle volume has always been thought to be important in relation to translocation<sup>29</sup>. For example, penetration by isotropic spherical particles becomes more difficult with increasing particle volume. However, for anisotropic particles undergoing physical penetration, as shown in Fig. 4b, the effect of particle volume is completely different. Indeed, particle penetration may be roughly

independent of particle volume, or even become easier with increasing particle volume. Similar observations are also obtained for larger particles (Supplementary Fig. S4). Therefore, the manner of increasing the particle volume for cargo loading is of vital importance.

As well as their geometry, penetration also depends on other particle properties. The chemical properties of the particle surface are an important factor. We find that by increasing the degree of hydrophobicity of the particle surface, the required force will decrease, but this tendency is non-monotonic (Supplementary Fig. S5). In addition, the initial velocity of the particle also affects particle penetration; although its role is not very distinct due to the 'softness' of

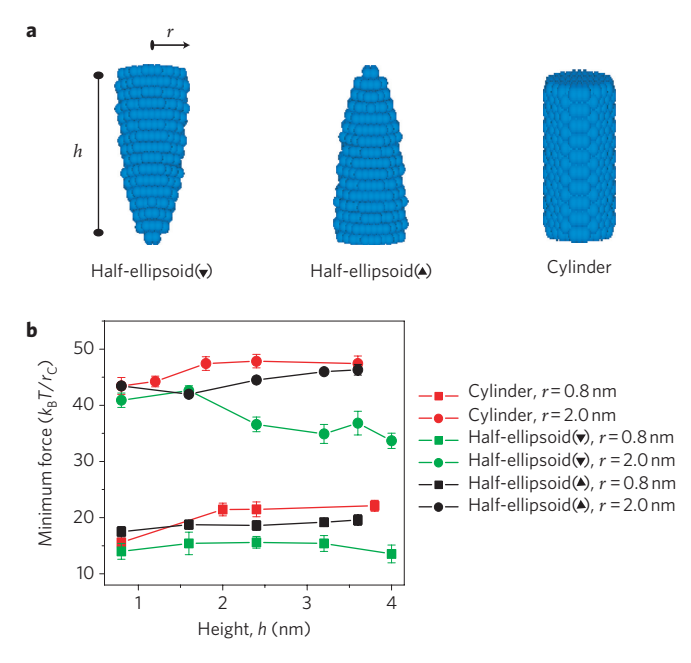


Figure 4 | Effects of particle disruption on translocation. **a**, Schematic showing three kinds of particles. 'Half-ellipsoid( $\mathbf{v}$ )' is the bottom half of the ellipsoid, 'half-ellipsoid( $\mathbf{A}$ )' is the upper half of the ellipsoid, and 'cylinder' represents a cylindrical particle. **b**, Graph showing minimum driving forces required to guide three kinds of particles of fixed radii (r = 0.8 nm and 2.0 nm) through the lipid bilayer at varying particle heights h.

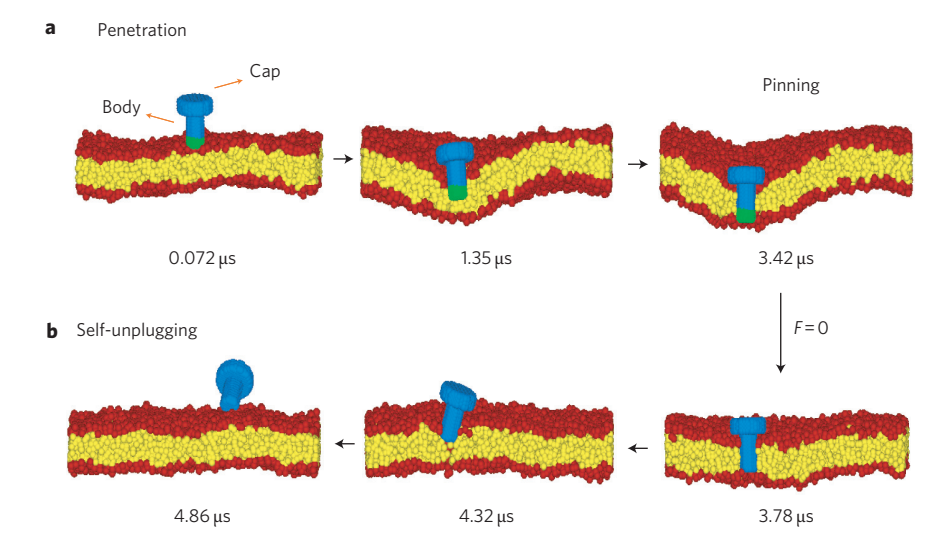


Figure 5 | Penetrating behaviour of pushpin-shaped particles. a,b, Computer-simulated image of evolving snapshots of the 'penetration' (a) and 'self-unplugging' (b) process of the pushpin-shaped particle. The green part of the particle (remainder in blue) represents the location of the driving force, where  $F = 24.5k_BT/r_c$ . The direction of the black arrows represents the sequence of snapshots over time. Pushpin cap radius,  $r_{cap} = 2.0$  nm; cap height,  $h_{cap} = 0.8$  nm. Pushpin body radius,  $r_{body} = 0.8$  nm; body height,  $h_{body} = 4.0$  nm. Red represents lipid heads, yellow represents lipid tails.

the bilayer, high particle velocity will benefit particle penetration (Supplementary Fig. S6).

In summary, the shape anisotropy and initial orientation of particles play a complicated role in their physical translocation, but their volume has only an indirect influence. Although these factors are usually coupled together, our findings indicate that if we can control the way the various shaped particles interact with the membrane, altering the geometry of particles can bring about new applications. For example, because having a larger volume may have little effect or even facilitate the entry of anisotropic particles into cells, it is possible to enhance the delivery efficiency of nanoscale carriers by changing their volume. Furthermore, by controlling the orientation of anisotropic particles, it is possible to improve the targeting of nanoparticles to specific cells. The shapes of particles may also help our understanding of the intricate interactions between biomacromolecules and the cell membrane. A typical example is the pushpin-shaped particle. With a particular orientation, this shape of particle could provide a new possible cargo delivery route for nanoparticles-it can 'pin' the lipid bilayer (Fig. 5a) and then self-unplug from the bilayer if the force is removed (Fig. 5b; see also Supplementary Fig. S7). In particular, it is helpful in understanding the behaviour of the transmembrane protein haemolysin, which interacts with the cellular membrane in a manner that is similar to the 'pinning' state<sup>30</sup>. Importantly, our results also provide new insights regarding receptor-mediated endocytosis. We find that the geometrical properties of particles, including their shape, volume and orientation, also affect the endocytosis process (Supplementary Figs S8-S12). Therefore, geometric considerations are important when designing a nanoparticle.

# Mathada

Dissipative particle dynamics (DPD) is a powerful mesoscopic simulation technology that allows the use of long time and length scales in simulations. Each DPD bead is composed of a group of atoms or molecules that are subject to three types of forces: conservative, dissipative and random. The motion of the bead obeys Newton's equation of motion (see Supplementary Information for details of the methods). Using DPD, we constructed a system comprising 3,950 lipids in enough water molecules (W). The lipid molecules were modelled as linear chains with two hydrophilic head beads (H) and five hydrophobic tail beads (T). They were assembled into a planar bilayer in a tensionless state, with the bilayer oriented in the x-y plane of the simulation box. As well as the lipids and water molecules, particles were also included in the simulation box. Each particle was fabricated by arranging the hydrophilic DPD beads (P) on an fcc lattice with a lattice constant of  $\alpha=0.28$  nm into a desired geometrical shape and volume; all beads forming a

particle moved as a rigid body. Owing to the close packing of the beads in the particle, water or other molecules were not able to enter the interior of the particle. At the beginning of the simulation, the particle was placed  $\sim\!1.6$  nm above the bilayer, and the system was then equilibrated while the location of the particle remained unchanged. A driving force F, directed in the z-direction, was applied to the centre of mass of the particle to aid its penetration across the bilayer. All simulations were performed in the canonical ensembles using a modified velocity–Verlet integration algorithm with a time step of  $\Delta t = 90$  ps, and each simulation time was at least 13.5  $\mu s$ . More details in this regard are presented in the Supplementary Information.

Received 7 April 2010; accepted 14 June 2010; published online 25 July 2010

# References

- Service, R. F. Nanotechnology takes aim at cancer. Science 310, 1132–1134 (2005).
- Xia, Y. Nanomaterials at work in biomedical research. *Nature Mater.* 7, 758–760 (2008).
- Mitragotri, S. & Lahann, J. Physical approaches to biomaterial design. Nature Mater. 8, 15–23 (2008).
- 4. Nel, A. *et al.* Understanding biophysicochemical interactions at the nano-bio interface. *Nature Mater.* **8,** 543–557 (2009).
- Decuzzi, P. & Ferrari, M. The receptor-mediated endocytosis of nonspherical particles. *Biophys. J.* 94, 3790–3797 (2008).
- Xia, T. et al. Comparison of the abilities of ambient and manufactured nanoparticles to induce cellular toxicity according to an oxidative stress paradigm. Nano Lett. 6, 1794–1807 (2006).
- Poland, C. A. et al. Carbon nanotubes introduced into the abdominal cavity of mice show asbestos-like pathogenicity in a pilot study. Nature Nanotech. 3, 423–428 (2008).
- Livadaru, L. & Kovalenko, A. Fundamental mechanism of translocation across liquidlike membranes: toward control over nanoparticle behavior. *Nano Lett.* 6, 78–83 (2006).
- Roiter, Y. et al. Interaction of nanoparticles with lipid membrane. Nano Lett. 8, 941–944 (2008).
- Obataya, I., Nakamura, C., Han, S., Nakamura, N. & Miyake, J. Nanoscale operation of a living cell using an atomic force microscope with a nanoneedle. *Nano Lett.* 5, 27–30 (2005).
- Wong-Ekkabut, J. et al. Computer simulation study of fullerene translocation through lipid membranes. Nature Nanotech. 3, 363–368 (2008).
- Qiao, R., Roberts, A. P., Mount, A. S., Klaine, S. J. & Ke, P. C. Translocation of C<sub>60</sub> and its derivatives across a lipid bilayer. *Nano Lett.* 7, 614–619 (2007).
- Wallace, E. J. & Sansom, M. S. P. Blocking of carbon nanotube based nanoinjectors by lipids: a simulation study. *Nano Lett.* 8, 2751–2756 (2008).
- Chen, X., Kis, A., Zettl, A. & Bertozzi, C. R. A cell nanoinjector based on carbon nanotubes. Proc. Natl Acad. Sci. USA 104, 8218–8222 (2007).

- Vakarelski, I. U., Brown, S. C., Higashitani, K. & Moudgil, B. M. Penetration of living cell membranes with fortified carbon nanotube tips. *Langmuir* 23, 10893–10896 (2007).
- Leroueil, P. R. et al. Wide varieties of cationic nanoparticles induce defects in supported lipid bilayers. Nano Lett. 8, 420–424 (2008).
- Hong, S. P. et al. Interaction of polycationic polymers with supported lipid bilayers and cells: nanoscale hole formation and enhanced membrane permeability. Bioconjugate Chem. 17, 728–734 (2006).
- Leroueil, P. R. et al. Nanoparticle interaction with biological membranes: does nanotechnology present a janus face? Acc. Chem. Res. 40, 335–342 (2007).
- Ginzburg, V. V. & Balijepailli, S. Modeling the thermodynamics of the interaction of nanoparticles with cell membranes. *Nano Lett.* 7, 3716–3722 (2007).
- Zasloff, M. Magainins, a class of antimicrobial peptides from Xenopus skin: isolation, characterization of two active forms and partial cDNA sequence of a precursor. *Proc. Natl Acad. Sci. USA* 84, 5449–5453 (1987).
- Cossart, P. Perspectives series: host/pathogen interactions. J. Clin. Invest. 99, 2307–2311 (1997).
- Champion, J. A. & Mitragotri, S. Role of target geometry in phagocytosis. Proc. Natl Acad. Sci. USA 103, 4930–4934 (2006).
- Gratton, S. E. A. et al. The effect of particle design on cellular internalization pathways. Proc. Natl Acad. Sci. USA 105, 11613–11618 (2008).
- Glotzer, S. C. & Solomon, M. J. Anisotropy of building blocks and their assembly into complex structures. *Nature Mater.* 6, 557–562 (2008).
- 25. Shillcock, J. C. & Lipowsky, R. Tension-induced fusion of bilayer membranes and vesicles. *Nature Mater.* **4**, 225–228 (2005).
- Laradji, M. & Kumar, P. B. S. Dynamics of domain growth in self-assembled fluid vesicles. *Phys. Rev. Lett.* 93, 198105 (2004).

- Schmidt, U., Guigas, G. & Weiss, M. Cluster formation of transmembrane proteins due to hydrophobic mismatching. *Phys. Rev. Lett.* 101, 128104 (2008).
- Alexeev, A., Uspal, W. E. & Balazs, A. C. Harnessing janus nanoparticles to create controllable pores in membranes. ACS Nano 2, 1117–1122 (2008).
- Jiang, W., Kim, B. Y. S., Rutka, J. T. & Chan, W. C. W. Nanoparticle-mediated cellular response is size-dependent. *Nature Nanotech.* 3, 145–150 (2008).
- 30. Song, L. Z. et al. Structure of staphylococcal-hemolysin, a heptameric transmembrane pore. Science 274, 1859–1865 (1996).

# Acknowledgements

The authors thank R. Austin, M. Laradji, I. Szleifer, Z. Zhang, W. Tian, C. Ren and X. Shi for helpful discussions. This work was supported by the National Basic Research Program of China under grant no. 2007CB925101 and the National Natural Science Foundation of China under grant no. 10974080.

#### **Author contributions**

K.Y. and Y.Q.M. conceived and designed the simulations. K.Y. and Y.Q.M. performed the simulations. K.Y. and Y.Q.M. analysed the data. K.Y. and Y.Q.M. co-wrote the paper. All authors discussed the results and commented on the manuscript.

### Additional information

The authors declare no competing financial interests. Supplementary information accompanies this paper at www.nature.com/naturenanotechnology. Reprints and permission information is available online at http://npg.nature.com/reprintsandpermissions/. Correspondence and requests for materials should be addressed to Y.Q.M.